



Two Dimensional Quantum Mechanical Scattering using Perfectly Matched Layers

A Major Qualifying Project

Submitted to the Faculty of the

WORCESTER POLYTECHNIC INSTITUTE

in partial fulfillment of the requirements for the

Degree of Bachelor of Science

By

Tyler K. Reynolds

Date: March 3, 2014

Advisor:

Prof. L. Ramdas Ram-Mohan

Department of Physics

Key Words: quantum mechanics, scattering, perfectly matched layers

Abstract

We consider a new way of looking at quantum mechanical scattering, motivated by the need for a framework that would allow calculations within complex waveguide geometries and for small scale systems. The two dimensional scattering problem is considered as a variational problem. This allows the use of the finite element method, which discretizes the region of interest so that numerical results may be obtained. We introduce stealth finite elements at the ends of a waveguide which serve to attenuate the wave. We demonstrate the numerical power of this framework by considering complicated scattering centers within wavefunctions. A modal analysis is performed on the resulting scattered waves.

Acknowledgements

The computational resources provided by the Center for Computational Nanoscience are greatly appreciated. Thanks to Kyle and my parents; I couldn't have gotten here without their support. Thanks also to Zehao Li, who helped me grasp the finer points of the finite element method.

Contents

Abstract	i
Acknowledgements	ii
Contents	iii
List of Figures	iv
1 Introduction	1
2 Scattering in Two Dimensions	3
2.1 The Source Term	3
2.2 Absorbing Boundary Conditions	4
3 Results and Discussion	6
3.1 Three Rows of Circular Scatterers	6
3.2 Randomly Placed Circular Scatterers	11
4 Summary and Future Work	20
4.1 Summary	20
4.2 Future Work	20
References	23

List of Figures

3.1	The mesh used for the FEM calculation of three rows of circular scattering centers. Scattering regions are shown in red, while stealth regions are displayed as green and propagation regions are displayed as blue.	6
3.2	The plot of the transmission coefficient versus the incident energy for three rows of circular scatterers. An incident plane wave in the mode $n = 1$ is shown. Only odd modes contribute to the total wave due to symmetry within the waveguide.	7
3.3	The plot of the transmission coefficient versus the incident energy for three rows of circular scatterers. An incident plane wave in the mode $n = 2$ is shown. Only even modes contribute to the total wave due to symmetry within the waveguide.	8
3.4	The plot of the transmission coefficient versus the incident energy for three rows of circular scatterers. An incident plane wave in the mode $n = 3$ is shown. Only odd modes contribute to the total wave due to symmetry within the waveguide.	9
3.5	The plot of the transmission coefficient versus the incident energy for three rows of circular scatterers. An incident plane wave in the mode $n = 4$ is shown. Only even modes contribute to the total wave due to symmetry within the waveguide.	10
3.6	The mesh used for the FEM calculation of randomly placed circular scatterers. Scattering regions are shown in red, while stealth regions are displayed as green and propagation regions are displayed as blue.	11
3.7	The plot of the transmission coefficient versus the incident energy for randomly placed circular scatterers. An incident plane wave in the mode $n = 1$ is shown. The odd modes are shown.	12

3.8	The plot of the transmission coefficient versus the incident energy for randomly placed circular scatterers. An incident plane wave in the mode $n = 1$ is shown. The even modes are shown.	13
3.9	The plot of the transmission coefficient versus the incident energy for randomly placed circular scatterers. An incident plane wave in the mode $n = 2$ is shown. The even modes are shown.	14
3.10	The plot of the transmission coefficient versus the incident energy for randomly placed circular scatterers. An incident plane wave in the mode $n = 2$ is shown. The odd modes are shown.	15
3.11	The plot of the transmission coefficient versus the incident energy for randomly placed circular scatterers. An incident plane wave in the mode $n = 3$ is shown. The odd modes are shown.	16
3.12	The plot of the transmission coefficient versus the incident energy for randomly placed circular scatterers. An incident plane wave in the mode $n = 3$ is shown. The even modes are shown.	17
3.13	The plot of the transmission coefficient versus the incident energy for randomly placed circular scatterers. An incident plane wave in the mode $n = 4$ is shown. The even modes are shown.	18
3.14	The plot of the transmission coefficient versus the incident energy for randomly placed circular scatterers. An incident plane wave in the mode $n = 4$ is shown. The odd modes are shown.	19

1 Introduction

In quantum mechanics, the wave nature of particles gives rise to a number of phenomena that are unseen in the realm of classical physics. Among these are the tunneling of particles through energy barriers and the scattering of particles off of potentials. Both of these phenomena have many applications, including the tunneling diode, the scanning tunneling microscope, and semiconductor heterostructures. In quantum mechanical scattering theory, waves come in from infinity and scatter off of a potential barrier. The resultant waves are detected at infinity. However, in nanoscale systems, these limits are not achieved. Furthermore, the solution to complicated scattering geometries cannot be easily found using the First Born Approximation and other familiar techniques from scattering theory. This motivates the need for a new method of looking at scattering problems.

We develop the problem of two-dimensional (2D) quantum mechanical scattering with the principle of stationary action. In this way, we are able to solve for the amplitude of the scattered wave. The mixed (Cauchy) boundary conditions that arise during this are difficult to implement computationally. To avoid this difficulty, we introduce perfectly matched layers (PMLs) outside of the scattering region. These layers act as absorbing or “stealth” regions, effectively attenuating the wave to zero. This allows us to reduce the Cauchy boundary conditions to Dirichlet boundary conditions. The concept of the perfectly matched layer is based on complex-coordinate stretching, in which a real function is continued onto the complex plane^[1]. PMLs have been used in areas including electromagnetic scattering, heat transfer, and elastic waves^[2, 3, 4] to great effect. They were first applied to quantum scattering theory by Ram-Mohan^[5], where they were called stealth elements.

For our calculations, we utilize the finite element method. Only recently has this powerful technique been applied to problems in quantum mechanics^[5]. This numerical method allows us to discretize the action within the region of interest. The use of interpolation polynomials for the wavefunction at nodal points on these elements generates the solution. In particular, the use of \mathcal{C}_1 -continuous interpolation polynomials gives increased numerical accuracy.

In Sec. 2, we develop the theory necessary to perform our calculations. We start by casting the scattering problem in a variational form and deriving the Cauchy boundary conditions. We then introduce stealth regions into our theory and determine the condition for no reflection from the interfaces between the scattering and stealth regions. In Sec. 3, results for scattering from a variety of scattering centers in a 2D waveguide are presented. Directions for future work are outlined and concluding remarks are given in Sec. 4.

2 Scattering in Two Dimensions

2.1 The Source Term

For our calculations, we want to generate plane waves of the form

$$G(x, y) = Ae^{ikx|x-x_0|}\phi(y). \quad (2.1)$$

Here, the term $\phi(y)$ represents a superposition of bound states for a particle in an infinite well. In order to create these waves, we place a line source at x_0 . We must add a source term to Schrödinger's equation so that it becomes

$$S\delta(x - x_0) = \nabla^2\psi(x, y) - k_0^2\psi(x, y), \quad (2.2)$$

where we have defined $k_0^2 = 2Em/\hbar^2$. We are able to separate Schrödinger's equation in 2D quite easily. We know that the contribution to the energy eigenvalues in the y-direction will be $k_y^2 = \hbar^2\pi^2n^2/2mL^2$, since the waveguide acts as an infinite well in the y-direction. We can therefore expand the Eq. 2.2 into

$$S\delta(x - x_0) = \left(\frac{\partial^2}{\partial x^2} + k_y^2 + k_0^2 \right) \psi(x, y). \quad (2.3)$$

We plug in $G(x, y)$ for $\psi(x, y)$ and integrate from $x_0 - \epsilon$ to $x_0 + \epsilon$. In the limit that ϵ goes to 0, we find that

$$S = 2Aik_x\phi(y), \quad (2.4)$$

where $k_x^2 = k_0^2 - k_y^2$. We now have the coefficient of the source term that will generate the plane waves we desire.

2.2 Absorbing Boundary Conditions

Consider the planar interface between the scattering region and the stealth region. We want to find the condition such that there is no reflection of the wave from this interface. Denote the scattering region by I and the stealth region as II. This will give rise to wavefunctions

$$\psi_I(x, y) = Ae^{i(k_{Ix}x+k_{Iy}y)} + Re^{-i(k_{Ix}x+k_{Iy}y)} \quad (2.5)$$

in the scattering region and

$$\psi_{II}(x, y) = Te^{i(k_{IIx}x+k_{IIy}y)} \quad (2.6)$$

in the stealth region. We introduce parameters a , b , and c , such that $a_I = b_I = c_I = 1$. The dispersion relation in region II gives us

$$\frac{1}{a_{II}}k_{IIx}^2 + b_{II}k_{IIy}^2 = c_{II}k_{II}^2. \quad (2.7)$$

Our requirement that the wavefunctions be continuous across the boundary gives us the condition that

$$(A + R)e^{ik_{Iy}y} = Te^{ik_{Iy}y}, \quad (2.8)$$

which reduces to $k_{Iy} = k_{IIy}$. Furthermore, from the condition that the derivative is continuous across the boundary, we find

$$ik_{Ix}(A - R) = \frac{ik_{IIx}}{a_{II}}T. \quad (2.9)$$

This allows us to eliminate the transmitted wave and obtain the ratio of the reflected amplitude to the incident amplitude as

$$\frac{R}{A} = \frac{k_{Ix} - k_{IIx}/a_{II}}{k_{Ix} + k_{IIx}/a_{II}}. \quad (2.10)$$

It's easy to see that the condition for no reflection is for $a_{II}k_{Ix} = k_{IIx}$. To enforce this, we set $b_{II} = c_{II} = a_{II}$ and let $a_{II} = 1 + i\alpha$, where α is the stealth parameter. The transmitted wave becomes

$$\psi(x, y) = T e^{ik_{Ix}x(i-\alpha)} e^{ik_{Iy}y}. \quad (2.11)$$

The stealth parameter α acts to attenuate the wave within the stealth region. A sufficient choice of α will ensure that the wave dies off quickly and in a continuous manner. Choosing a discontinuous function for α could cause reflections.

3 Results and Discussion

In what follows, plane waves are incident upon scattering centers in a waveguide. Electrons are chosen as the particle, and we set $m^* = 0.067m_0$, which coincides with the mass ratio of an electron in a conduction band of a GaAs medium. The waveguides have a height of 300 Å.

3.1 Three Rows of Circular Scatterers

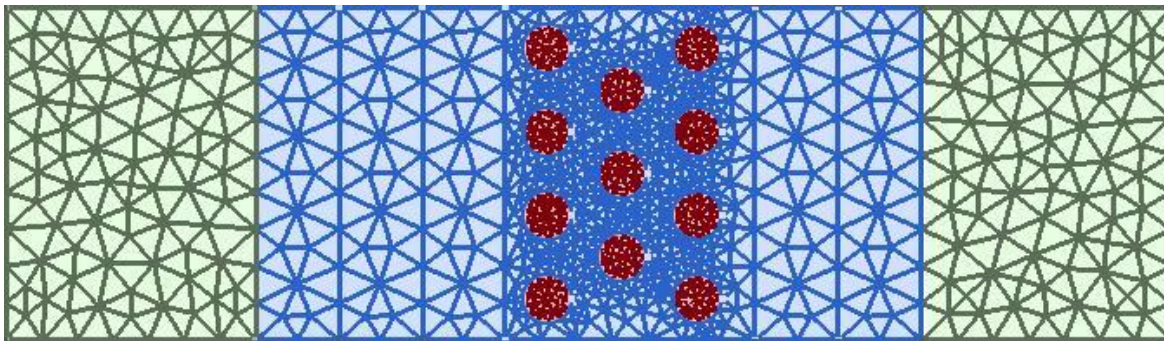


Figure 3.1: The mesh used for the FEM calculation of three rows of circular scattering centers. Scattering regions are shown in red, while stealth regions are displayed as green and propagation regions are displayed as blue.

The mesh presented in Fig. 3.1 consists of three rows of circular scatterers. Each scatterer has an energy of 300 meV. It is challenging to find an analytical solution for this geometry using the traditional methods of perturbation theory and the First Born Approximation. With the finite element method, we are able to obtain a solution for this system. Plane waves with modes up to $n = 4$ were incident on the array of scatterers. Due to the symmetry within the waveguide, it can be seen that only odd modes contribute to the total wave when n is odd, and similarly for the case when n is even.

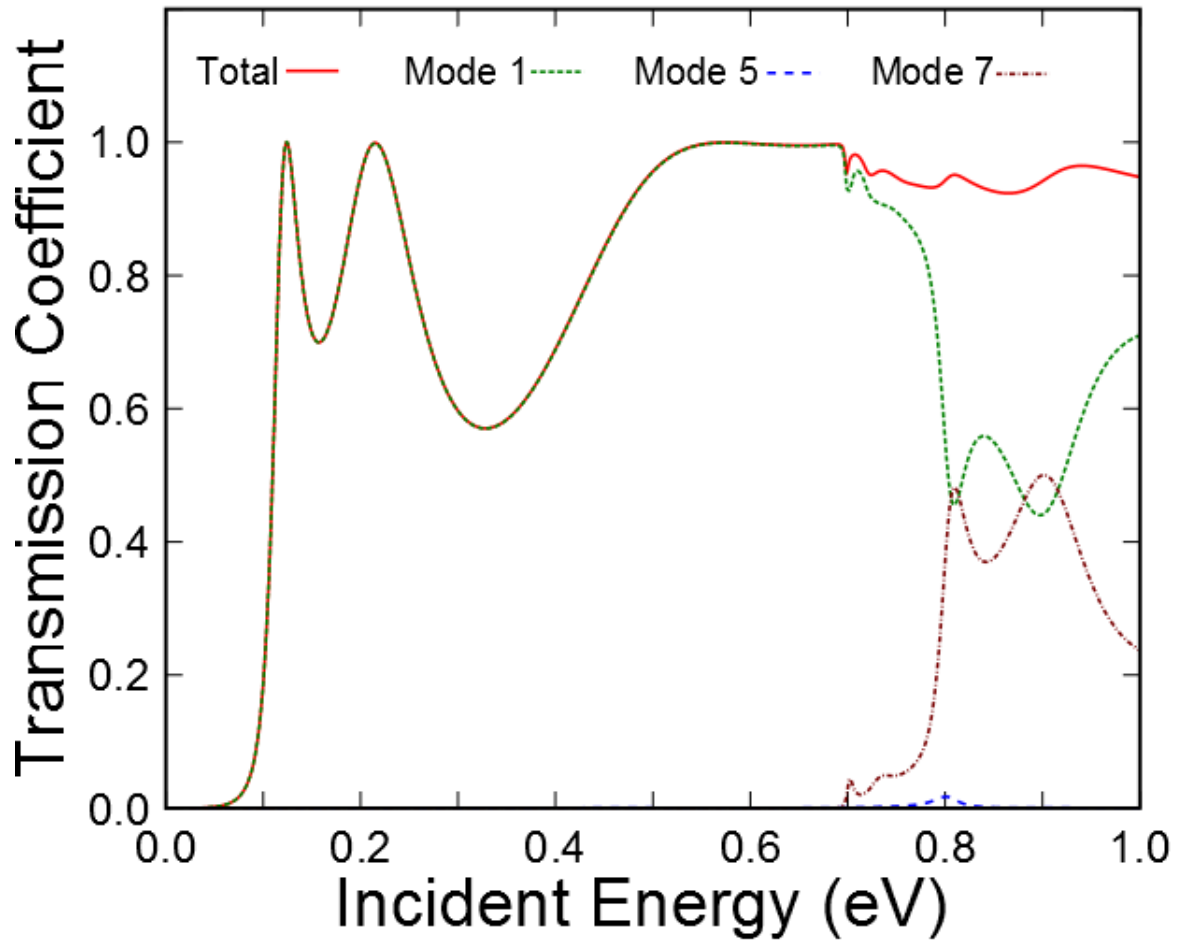


Figure 3.2: The plot of the transmission coefficient versus the incident energy for three rows of circular scatterers. An incident plane wave in the mode $n = 1$ is shown. Only odd modes contribute to the total wave due to symmetry within the waveguide.

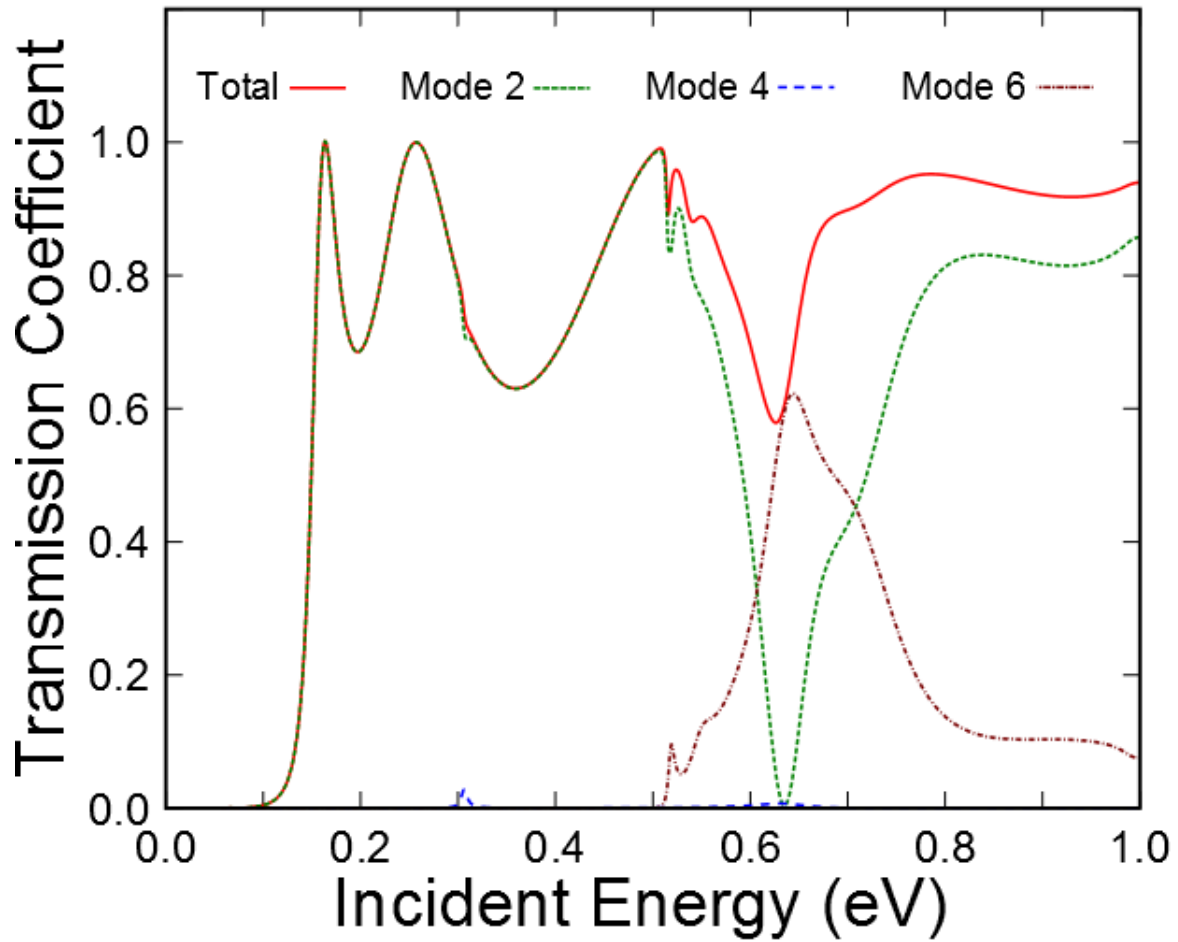


Figure 3.3: The plot of the transmission coefficient versus the incident energy for three rows of circular scatterers. An incident plane wave in the mode $n = 2$ is shown. Only even modes contribute to the total wave due to symmetry within the waveguide.

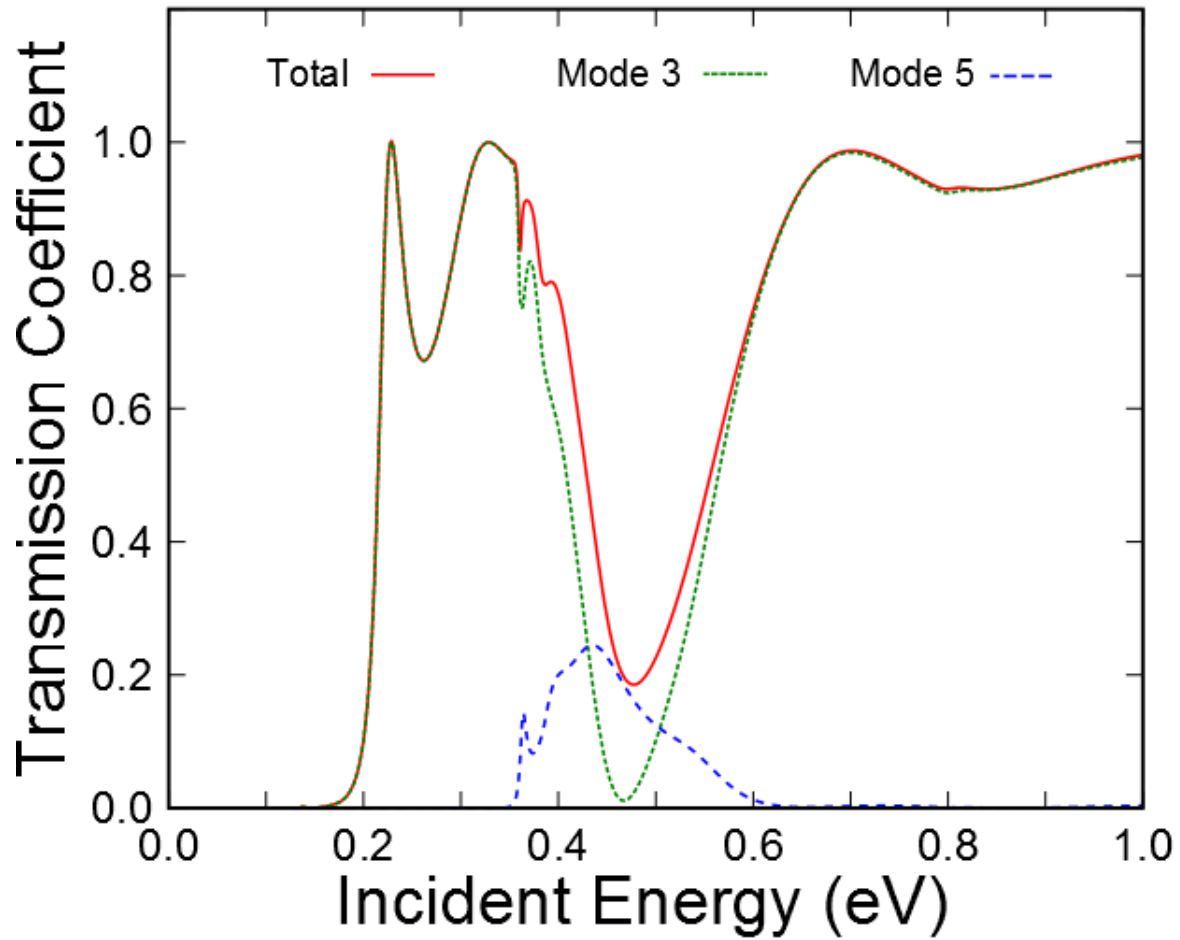


Figure 3.4: The plot of the transmission coefficient versus the incident energy for three rows of circular scatterers. An incident plane wave in the mode $n = 3$ is shown. Only odd modes contribute to the total wave due to symmetry within the waveguide.

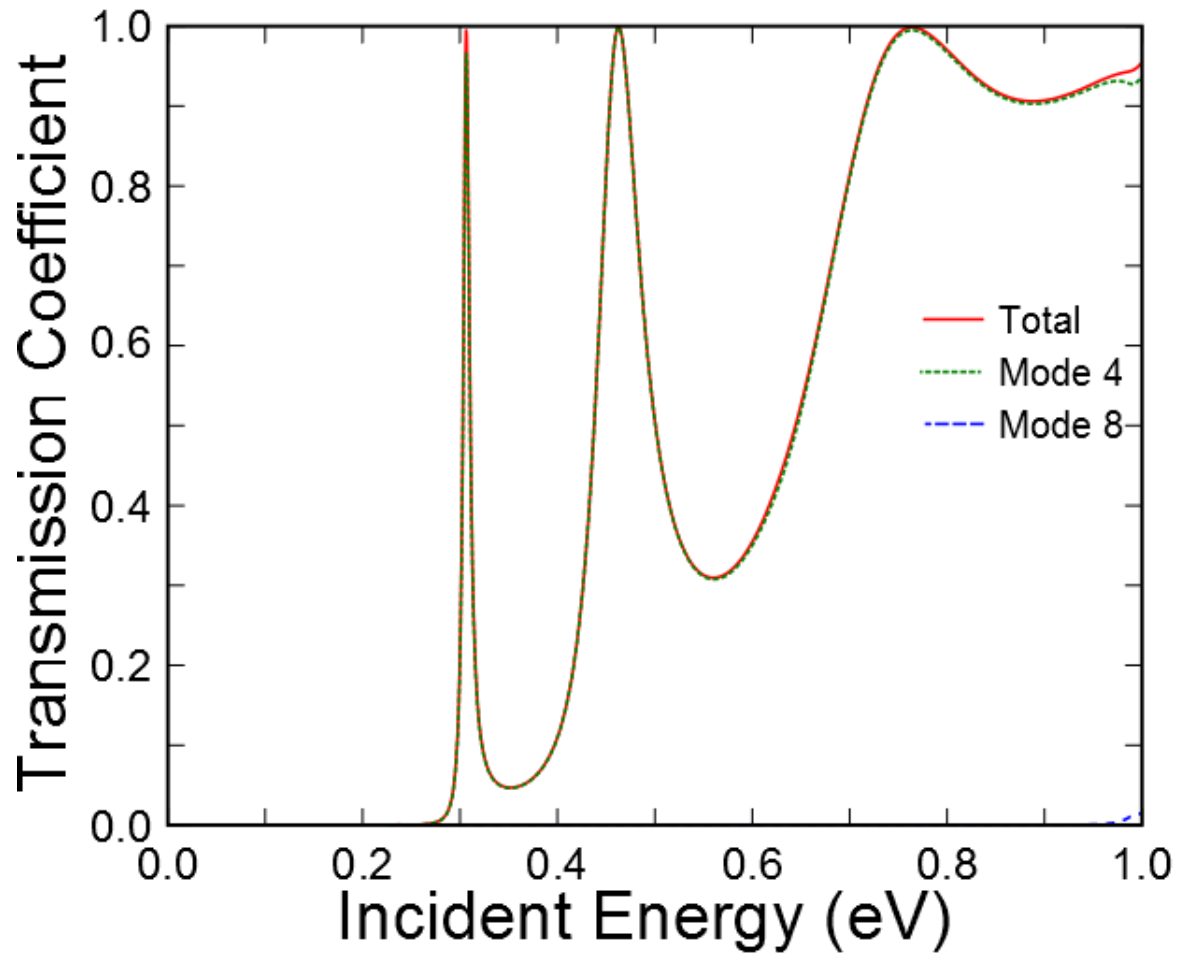


Figure 3.5: The plot of the transmission coefficient versus the incident energy for three rows of circular scatterers. An incident plane wave in the mode $n = 4$ is shown. Only even modes contribute to the total wave due to symmetry within the waveguide.

3.2 Randomly Placed Circular Scatterers

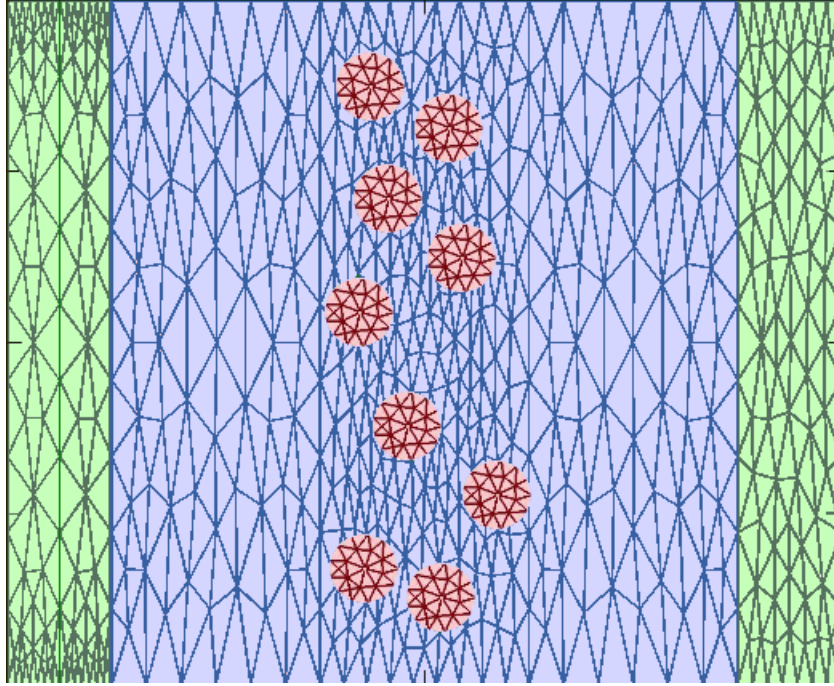


Figure 3.6: The mesh used for the FEM calculation of randomly placed circular scatterers. Scattering regions are shown in red, while stealth regions are displayed as green and propagation regions are displayed as blue.

We now consider randomly placed circles in a waveguide, as shown in Fig. 3.6. The circles all have equal radii of 10 \AA and each has an energy of 300 meV . The circles were arranged in a manner such that no circle was within a distance of two radii of another circle. Plane waves were incident upon the scatterers with modes up to $n = 4$. It can be seen in the transmission versus incident energy plots that all modes contribute to the total wave in this case, due to the loss of symmetry from the randomized positions of the circles.

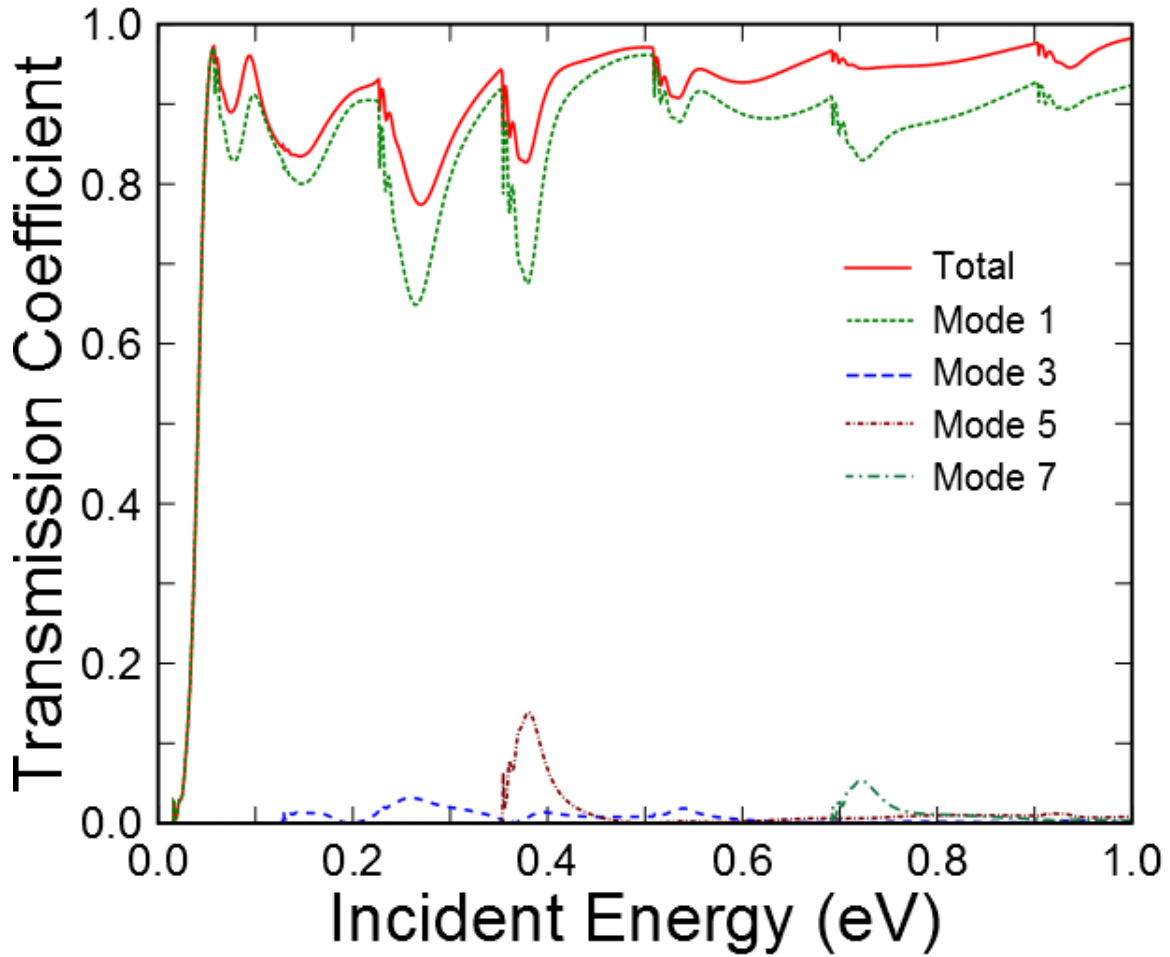


Figure 3.7: The plot of the transmission coefficient versus the incident energy for randomly placed circular scatterers. An incident plane wave in the mode $n = 1$ is shown. The odd modes are shown.

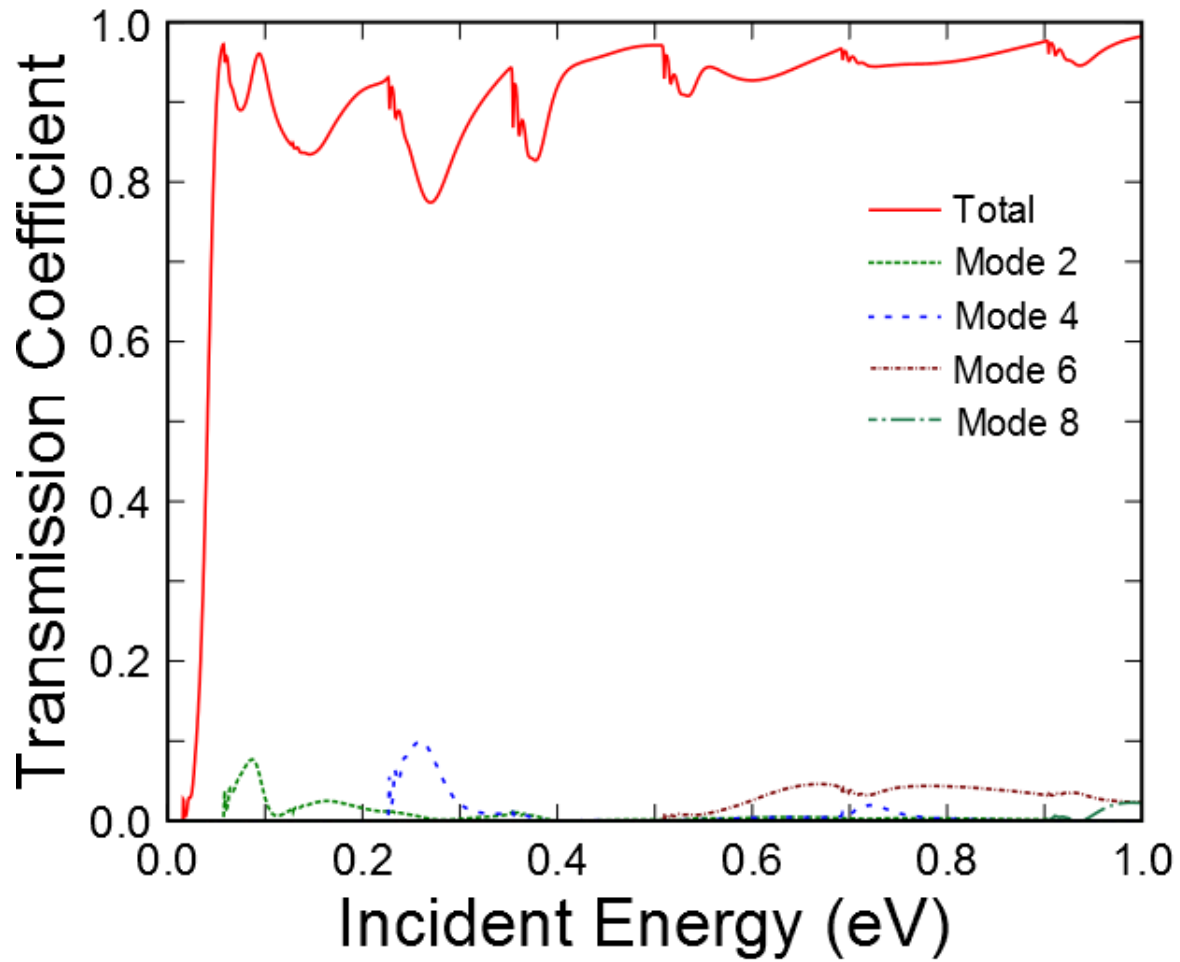


Figure 3.8: The plot of the transmission coefficient versus the incident energy for randomly placed circular scatterers. An incident plane wave in the mode $n = 1$ is shown. The even modes are shown.

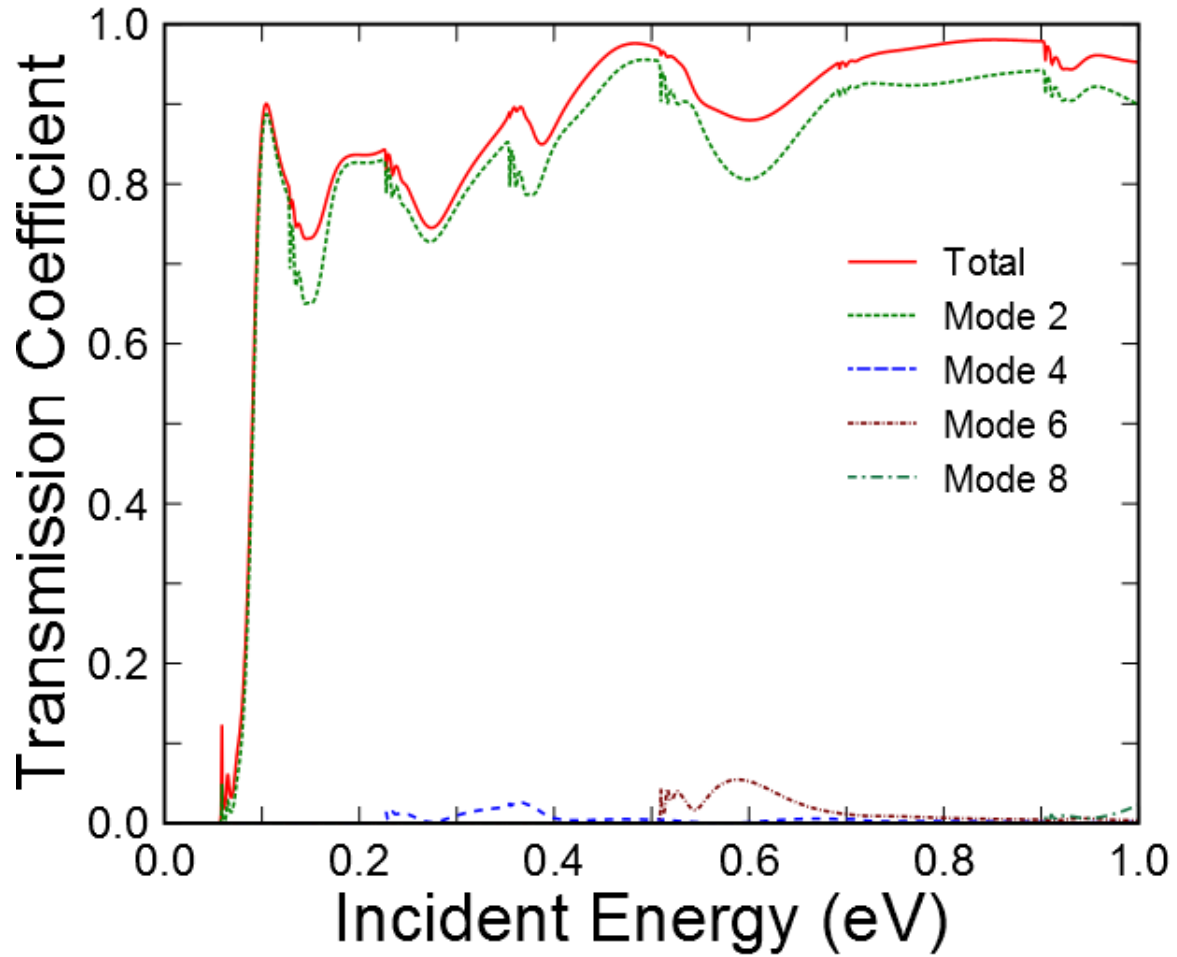


Figure 3.9: The plot of the transmission coefficient versus the incident energy for randomly placed circular scatterers. An incident plane wave in the mode $n = 2$ is shown. The even modes are shown.

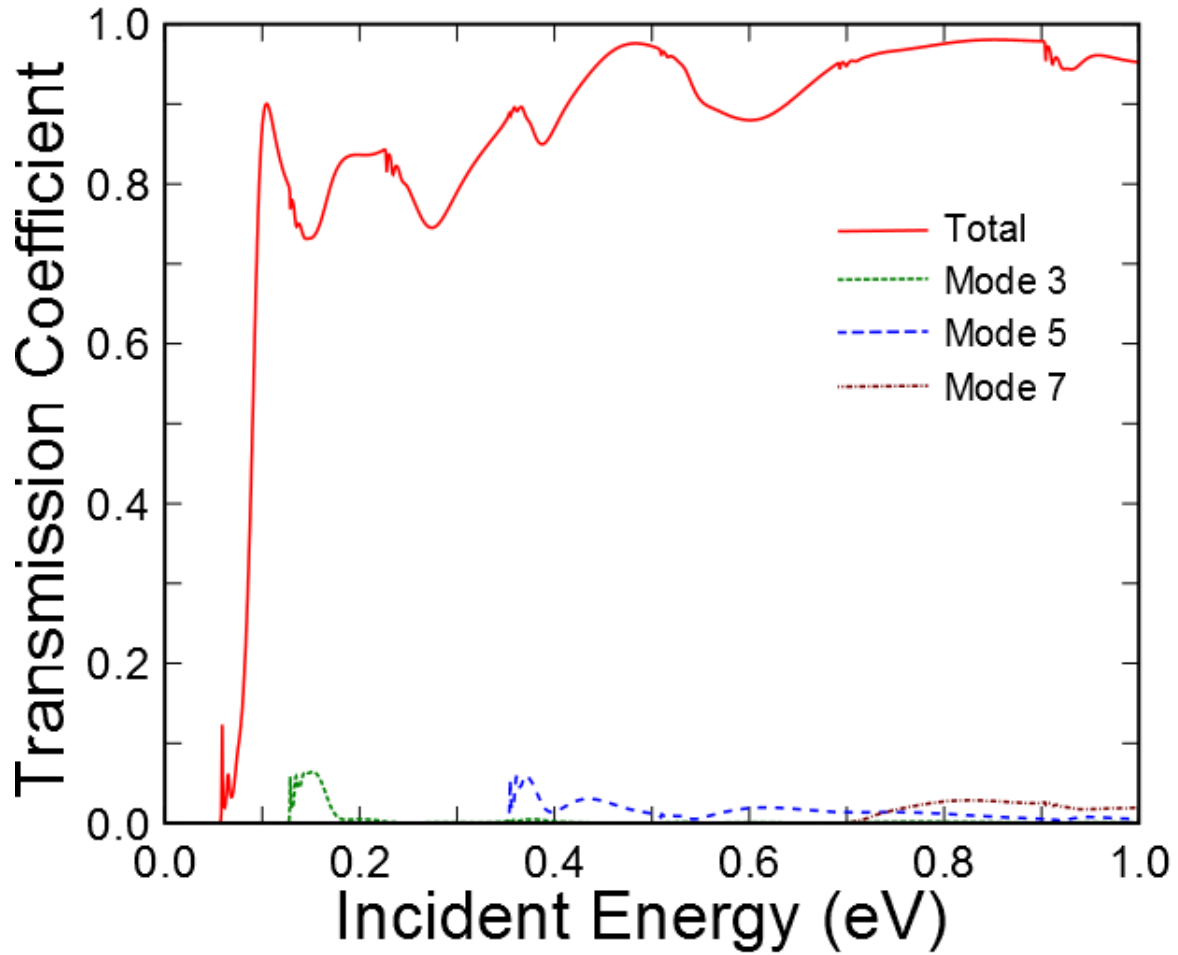


Figure 3.10: The plot of the transmission coefficient versus the incident energy for randomly placed circular scatterers. An incident plane wave in the mode $n = 2$ is shown. The odd modes are shown.

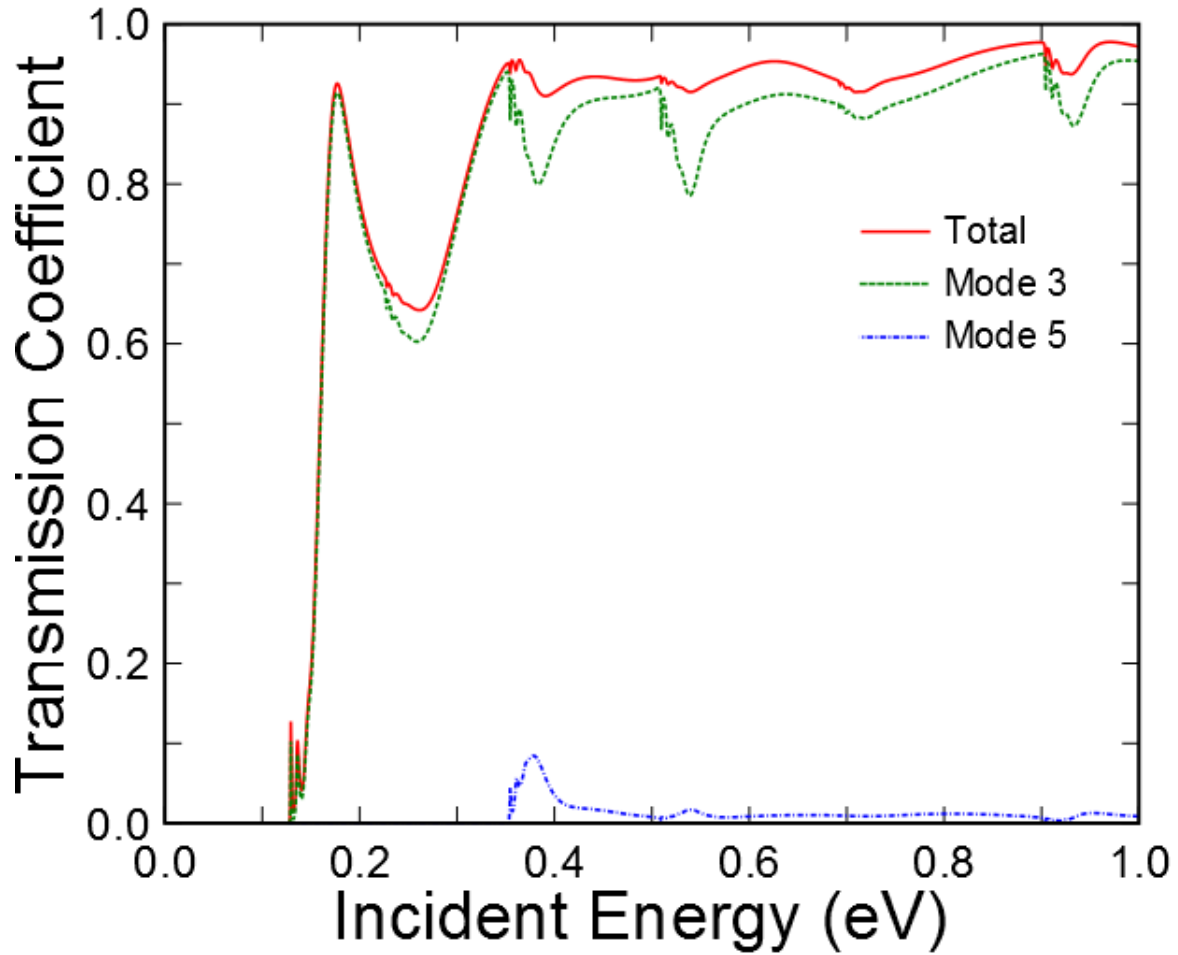


Figure 3.11: The plot of the transmission coefficient versus the incident energy for randomly placed circular scatterers. An incident plane wave in the mode $n = 3$ is shown. The odd modes are shown.

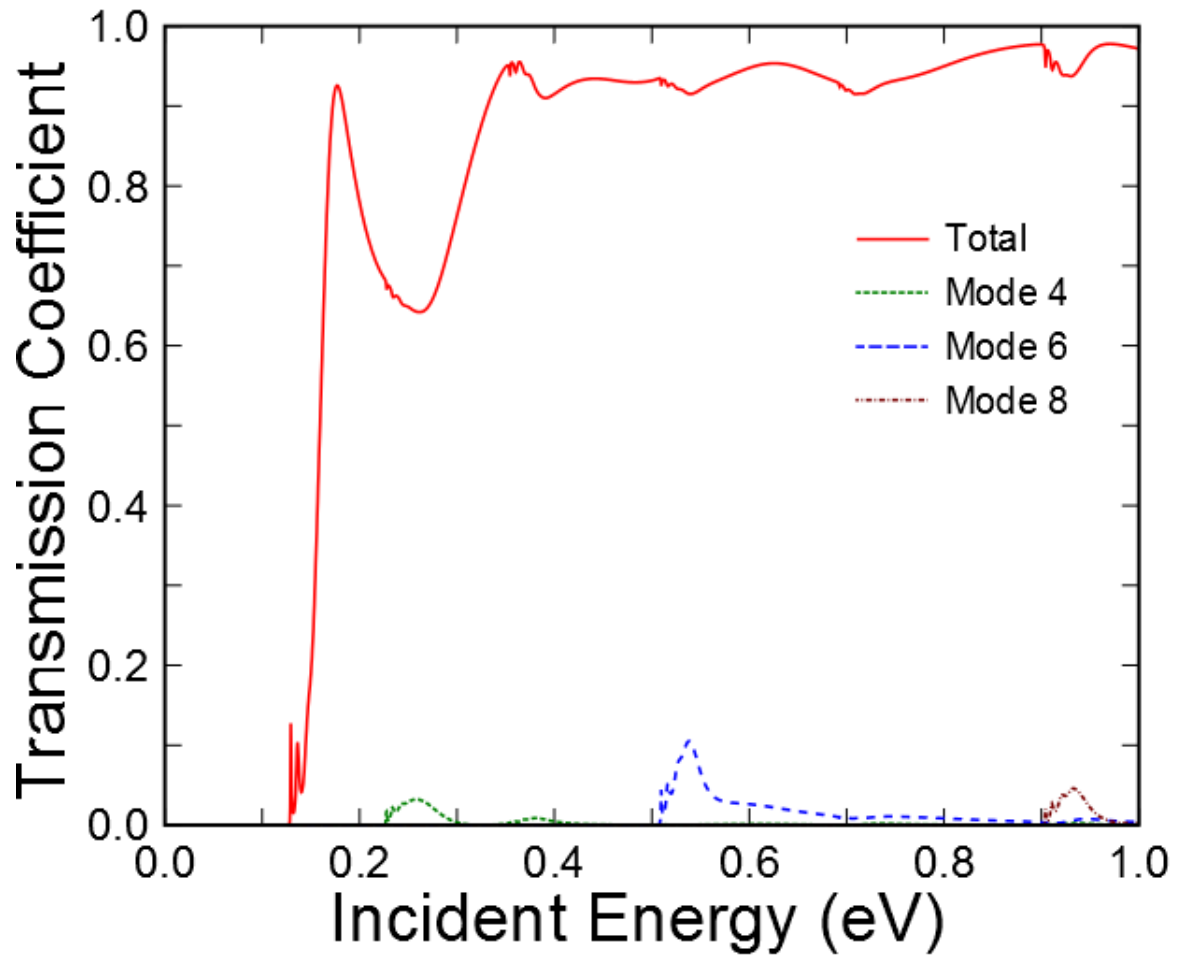


Figure 3.12: The plot of the transmission coefficient versus the incident energy for randomly placed circular scatterers. An incident plane wave in the mode $n = 3$ is shown. The even modes are shown.

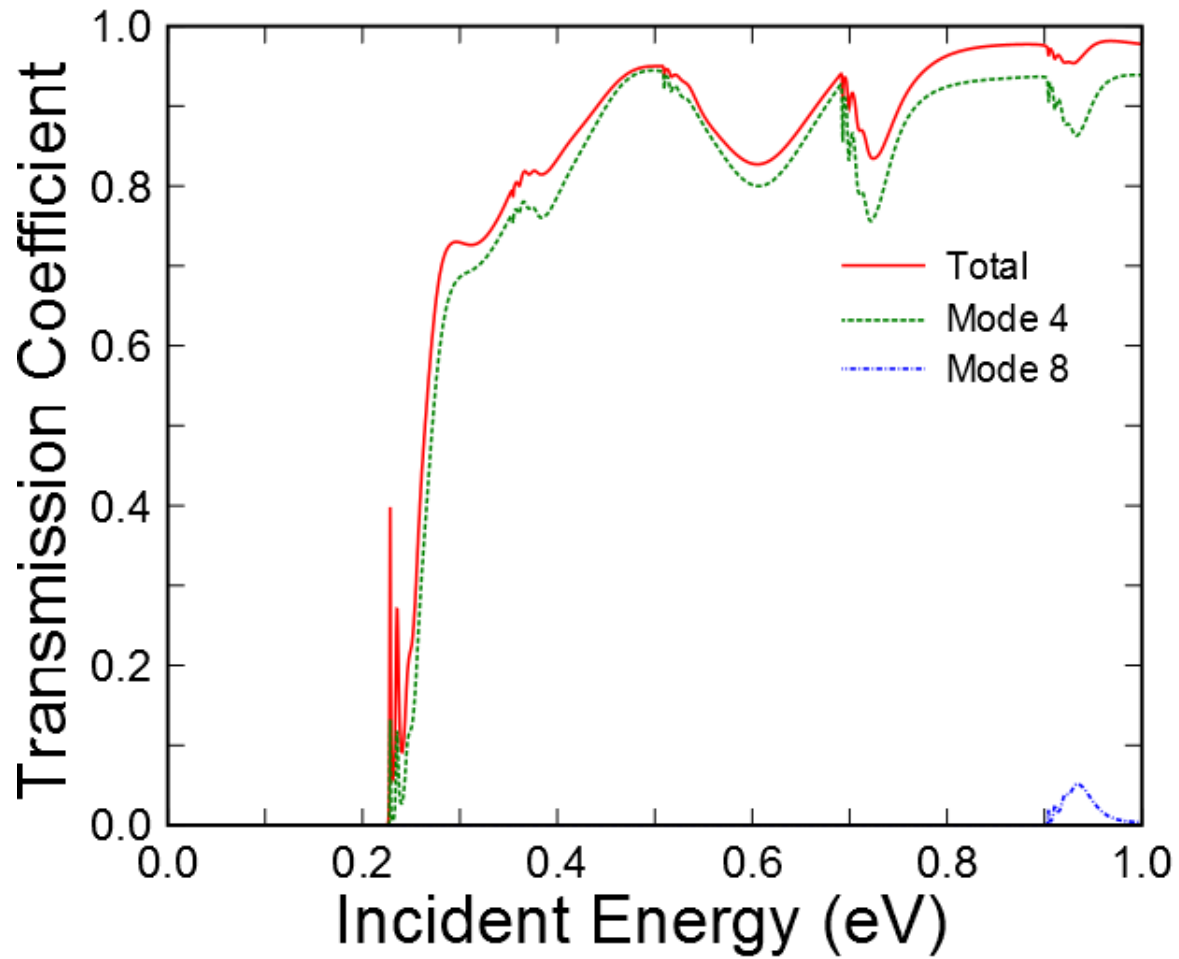


Figure 3.13: The plot of the transmission coefficient versus the incident energy for randomly placed circular scatterers. An incident plane wave in the mode $n = 4$ is shown. The even modes are shown.

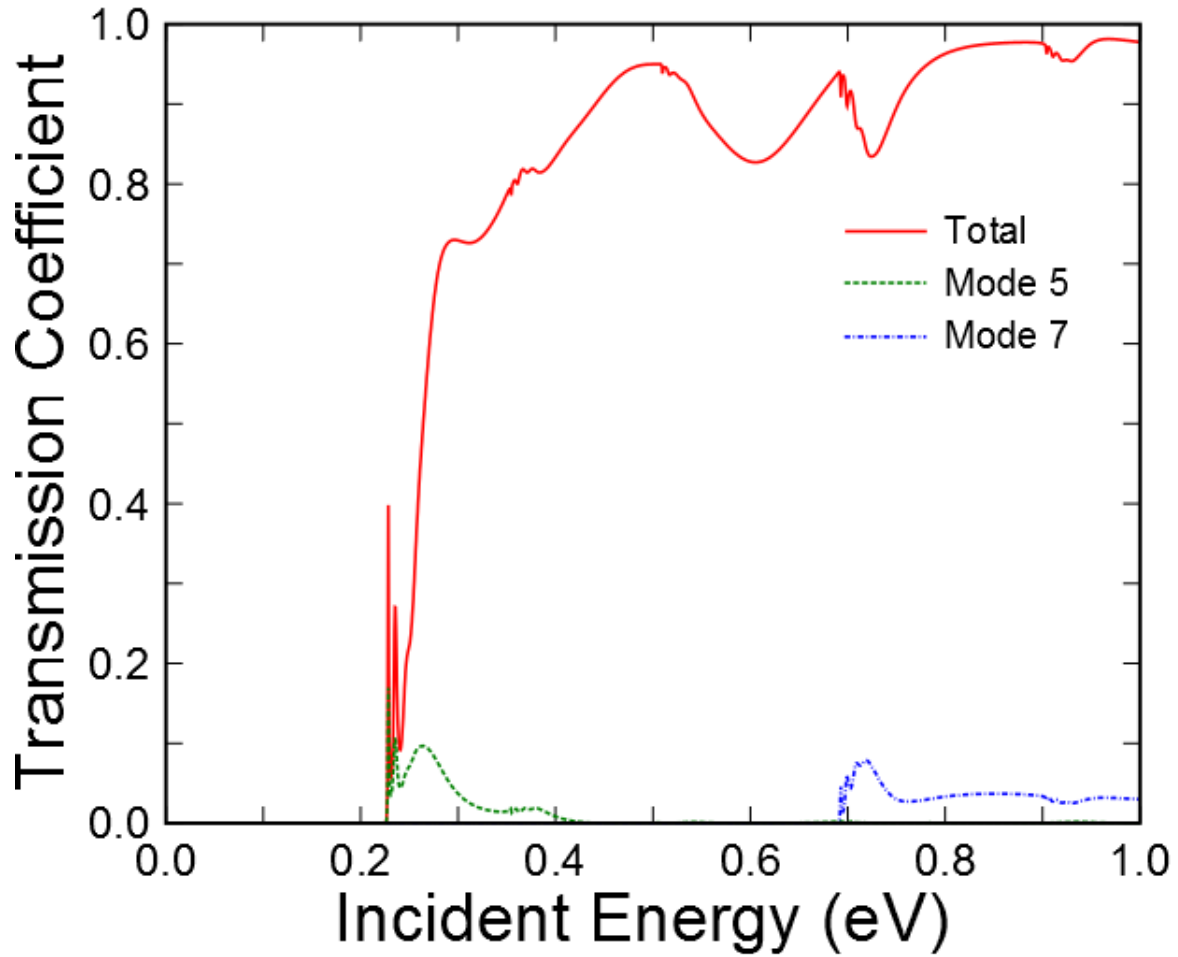


Figure 3.14: The plot of the transmission coefficient versus the incident energy for randomly placed circular scatterers. An incident plane wave in the mode $n = 4$ is shown. The odd modes are shown.

4 Summary and Future Work

4.1 Summary

The treatment of quantum mechanical scattering given here is important for the modeling of systems with complicated geometries or small scales. Usually in scattering theory, waves come in from infinity and are scattered out to infinity. On smaller scales, however, this limit is never attained. With complicated geometries, the energy is not easily separable and it is difficult, or sometimes impossible, to obtain an analytical solution. Using the finite element method helps to model these systems and provide accurate results.

In this paper, we started by recasting the problem of quantum mechanical scattering in a variational form. This allowed us to work within the framework of the finite element method. We also used a source term to control the incident wave introduced into the system. The introduction of stealth elements around the scattering region allowed us to reduce the Cauchy boundary conditions we obtained to simpler Dirichlet boundary conditions. These layers introduced a stealth parameter α , which attenuated the wave once it had crossed into the stealth region. For our finite element calculations, we worked with \mathcal{C}_1 -continuous interpolation polynomials, giving a higher degree of accuracy in the results. We calculated the transmission coefficient versus the incident energy for several scattering geometries within a waveguide.

4.2 Future Work

Scattering in the open domain in 2D remains to be pursued. The entire scattering regions will be surrounded by stealth regions so as to attenuate the wave in all directions. The outgoing waves will be given by Hankel functions of the first kind. It may be beneficial to surround the region with a circular stealth region, so that the stealth parameter depends on the radial distance instead of linear distance. This would help avoid any possible complications that would arise from sharp corners.

Furthermore, scattering in 3D remains to be explored. In the 3D case, tetrahedral elements will be used. There will be a substantial increase in the matrix sizes in the finite element calculations, necessitating more computing power. It will be very important for the codes that handle the 3D case to use parallelization and be highly optimized.

References

- [1] W.C. Chew, J.M Jin, and E. Michielssen. Complex coordinate stretching as a generalized absorbing boundary condition. *Microwave and Optical Technology Letters*, 15(6):363–369, August 1997.
- [2] Korada Umashankar and Allen Taflove. A novel method to analyze electromagnetic scattering of complex objects. *IEEE Transactions on Electromagnetic Compatibility*, EMC-24(4):397–405, November 1982.
- [3] Nicolas Lantos and Frédéric Nataf. Perfectly matched layers for the heat and advection-diffusion equations. *C. R. Acad. Sci. Paris, Ser. I*, 348:781–785, 2010.
- [4] Q.H. Liu. Perfectly matched layers for elastic waves in cylindrical and spherical coordinates. *J. Acoust. Soc. Am.*, 105(4):2075–2084, April 1999.
- [5] L.R. Ram-Mohan. *Finite Element and Boundary Element Applications in Quantum Mechanics*. Oxford U.P., Oxford, UK, 2002.
- [6] D.J. Griffiths. *Introduction to Quantum Mechanics*. Prentice Hall, NJ, 1st edition, 1995.
- [7] J.R. Taylor. *Scattering Theory: The Quantum Theory of Nonrelativistic Collisions*. Dover, NY, 2006.
- [8] T.N. Rescigno, C.W. McCurdy Jr., and A.E. Orel. Extensions of the complex-coordinate method to the study of resonances in many-electron systems. *Phys. Rev. A*, 17(6):1931–1938, June 1978.
- [9] C. William McCurdy, Carrie K. Stroud, and Matthew K. Wisinski. Solving the time-dependent schrödinger equation using complex-coordinate contours. *Phys. Rev. A*, 43(11):5980–5990, June 1991.

- [10] Julia Turner and C. William McCurdy. The application of exterior complex scaling in calculations on resonances in nuclear motion in molecular systems. *Chemical Physics*, 71:127–133, 1982.
- [11] M.L. Goldberger and K.M. Watson. *Collision Theory*. J. Wiley and Sons, NY, 1964.
- [12] Andrei V. Ilyashenko. Quantum mechanical scattering with absorbing boundaries.
- [13] D. Bohm. *Quantum Theory*. Dover, NY, 1989.
- [14] Steven G. Johnson. Notes on perfectly matched layers (pmls).
- [15] Philip F. Bagwell. Evanescent modes and scattering in quasi-one-dimensional wires. *Phys. Rev. B*, 41(15):10354–10371, May 1990.
- [16] Andrew F. Peterson. Vector finite element formulation for scattering from two-dimensional heterogeneous bodies. *IEEE Transactions on Antennas and Propagation*, 43(3):357–365, March 1994.